Stability Analysis of the Kármán Boundary-Layer Flow

Yun-Yong Lee* and Young-Kyu Hwang**

Key words: Kármán boundary-layer flow, Hydrodynamic stability, Rotating disk flow, Disturbance amplification

Abstract

The Kármán boundary-layer has been numerically investigated for the disturbance wave number, wave velocity, azimuth angle and radius (Reynolds number, Re). The disturbed flow over rotating disk can lead to transition at a much lower Re than that of the well-known Type I instability. This early transition is due to the excitation of the Type II. Presented are the neutral stability results concerning these instabilities by solving newly formulated stability equations with consideration of whole convective terms. When the present numerical results are compared with the previously known results, the value of critical Re corresponding to Type I is moved from $Re_{c,1}=285.3$ to 270.2 and the value corresponding to Type II is from $Re_{c,2}=$ 69.4 to 36.9, respectively. Also, the corresponding wave number is moved from $k_1=0.378$ to 0.386 for Type I; from $k_2=0.279$ to 0.385 for Type II. For Type II, the upper limit of wave number and azimuth angle is $k_U=0.5872$, $\varepsilon_U=-17.5°$, while its lower limit is near $k_U=0$, $\varepsilon_U\approx-28.4°$. This implies that the disturbances will be relatively fast amplified at small Re and within narrow bands of wave number compared with the previous results.

Nomenclature

C : $\cos\varepsilon$
Co : Coriolis parameter, $2-\mathrm{Ro}-\mathrm{Ro}^2$
Cp : wave velocity, β/k
D : characteristic boundary-layer thickness, $\sqrt{\nu/\Omega}$
J : scaling factor, [$O(1)$]
r : non-dimensional radius, $\bar{r}/D$
Re : Reynolds number, $\Delta\omega\bar{r}D/\nu$
Ro : Rossby number, $\Delta\omega/\Omega$ (for Kármán boundary-layer, Ro$=-1$)
S : $\sin\varepsilon$
z : non-dimensional axial coordinates, $\bar{z}/D$

Greek symbols

k : complex wave number, $\bar{k}D$
β : complex frequency, $\bar{\beta}/\omega_D$

* Research Associate, School of Mechanical Engineering, Sungkyunkwan University, Suwon 440-746, Korea
** School of Mechanical Engineering, Sungkyunkwan University, Suwon 440-746, Korea

δ : rotating angle of new oriented coordinate, $\varepsilon+(\pi/2)$
ε : azimuthal angle of disturbances
ξ : radial components of perturbation vorticity equation
η : tangential components of perturbation vorticity equation
η_∞ : outer of the boundary-layer
ν : kinematic viscosity [cm^2/sec]
$\Delta\omega$: a relative angular speed of fluid, $\omega_F-\omega_D$
ω_F : angular velocity of fluid
ω_D : angular velocity of disk

Superscripts

$-$: dimensional variable
$\hat{}$: new oriented curvilinear coordinates

Subscripts

c : critical
I : imaginary
R : real
∞ : outer region of the boundary-layer
1 : Type I instability
2 : Type II instability

1. Introduction

The hydrodynamic stability over the rotating system has been investigated by many scientists in order to understand the fundamental mechanism of 3-dimensional boundary-layer transition process (Faller,[1] Kobayashi et al.,[2] Kohama and Suda,[3] Lilly,[4] Lingwood,[5] Malik,[6] Smith[7] and Wilkinson and Malik[8]). Various types of flows belong to this category. As an example, the stability and transition of rotating flows have been related to aerospace, marine applications and similar phenomena over swept-back airfoils such as an impeller, transition process of ICBM's cone and electron devices of wafer.

The rotation of flow system dramatically affects the stability characteristics of flows at various physical situations. After the famous exact solution for the Kármán boundary-layer flow were obtain by Sparrow and Gregg,[9] the progress made in stability theory and experiment for rotating flows has been explosive in the past decades. The stability analyses of Lilly[4] and Faller and Kaylor[10] for the Ekman and Kármán boundary-layer flow revealed that the inclusion of Coriolis term in the stability analysis for stationary disturbance wave yields the significant increment of the critical Reynolds number, $\mathrm{Re}_{c,1}$ (i.e., Type I instability). Also, they found that another mode of instability (i.e., Type II instability) for moving disturbance waves, caused by the Coriolis force, exists at much lower value of critical Reynolds number, $\mathrm{Re}_{c,2}$ compared to those of stationary disturbance waves for the Kármán boundary-layer.

Some examples of the stationary disturbances are concerned with the Type I instability described as below. The boundary-layer flow over a rotating disk in a quiescent fluid has frequently been used as a canonical three-dimensional flow that amplifies the cross-flow instability. In this flow, the instability appears as outward-spiraling vortices. The Kármán boundary-layer transition on a rotating disk was first studied by Smith[7] using the hot-wire technique. He observed that sinusoidal disturbances appear in the disk boundary-layer at sufficiently large Reynolds numbers. Approximately 32 oscillations were observed within a disk rotation period and his numerical analysis indicated that the disturbances propagate at an angle of about 14° relative to the outward drawn radius (where the direction of disk rotation defines positive angle). Later, Gregory et al.[11] observed 28~31 spiraling outward vortices over a rotating disk at an angle of about 14° by using the china-clay technique for flow

visualization. These vortices, which appeared stationary relative to a disk, were first observed at the local Reynolds number Re≃430, transition to turbulence occurred near Re≃530 (see also Gregory and Walker[12]). The stationary disturbance wave established in a rotating disk was subsequently studied by lots of investigators. Kobayashi et al.[2] performed a theoretical analysis in which some of the effects of Coriolis and streamline curvature were considered. They calculated the value of $Re_{c,1}$ as 261 and observed that the number of spiral vortices is 31 or 32 at the position of Re≃297 and that the gradient of vortex axis was decreased from 14° to 7° as Re was increased. Malik et al.[13] numerically predicted that the critical Reynolds number $Re_{c,1}$ for establishment of stationary disturbance wave is 287 and these vortices spiral outward at an angle of about $\varepsilon_{c,1}=11.2°$ (Note that the recalculated values of Malik[6] are $Re_{c,1}=285.36$ and $\varepsilon_{c,1}=11.4°$). They observed that there were about 21 vortices at Re≃294. Similarilly, their calculated value of $Re_{c,2}$ for Type II moving disturbance wave for the Ekman boundary-layer was about 49.

For the Kármán boundary-layer flow, Faller[1] considered the effects of Coriolis force and streamline curvature in his stability analysis and obtained the neutral stability results, e.g., $Re_{c,1}=285.3$, $k_{c,1}$ (wave number at $Re_{c,1}$)= 0.378 and $\varepsilon_{c,1}$ (azimuth angle at $Re_{c,1}$)=13.9° for Type I instability, while $Re_{c,2}=69.4$, $k_{c,2}=0.279$ and $\varepsilon_{c,2}=-19°$ for Type II instability. He took sequential photographs of dye bands which were moving outward, as seen in Fig. 1(a). The resulting sketches of die patterns in Fig. 1(b) illustrated the typical structures of Type II and secondary instabilities.

The present study is a stability analysis of rotating disk flow (i.e., the Kármán boundary-layer), in which the effects of Coriolis force and streamline curvature are included. The previously known linear stability equations of Faller[1] are reformulated by correcting sign errors and by keeping whole convective terms. Using the orthogonal collocation technique accurately solves the reformulated stability equations. The results yield more complete 4-dimensional neutral stability curves, corresponding to the Type I and II instabilities, than those of previous investigators. It will be seen that the flow is always stable for a disturbance whose dimensionless wave number k is greater than 0.8 (i.e., if $\omega_D=0.325$ rps, and whose corresponding physical wave number $\bar{k}>4.27$ cm^{-1}). It will also be shown that the azimuth angle of disturbance wave which spiral outward tend to be decreased from 13.2° to lower angle as the local Reynolds number is further

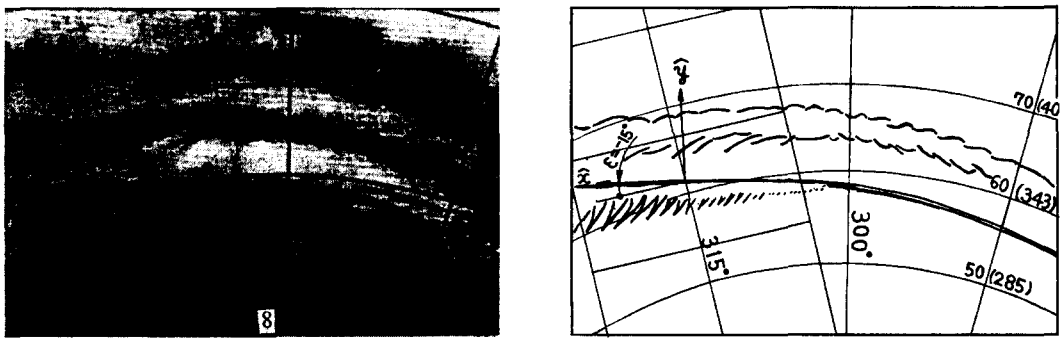

(a) Photo from Faller[1] (b) Sketch of their structured

Fig. 1 Type II and secondary instability of Kármán boundary-layer illustrated.

increased from $Re_{c,1}$. Otherwise the first unstable condition for Type II instability mode is the band of dimensionless wave numbers $0.0 \leq k \leq 0.587$ with azimuth angles $-28.4° \leq \epsilon \leq -17.5°$.

2. The governing equations and numerical method

2.1 Base flow equation

The model presented here describes a family of boundary-layer flows caused by a differential rotation rate between a solid boundary, or disk, and an incompressible fluid in rigid-body rotation (see Faller[1]). Particular cases of this family are the Kármán, Ekman and Bödewadt boundary-layer flows. The radius of the disk and the extent of the fluid above the disk are considered to be infinite, and the disk and fluid rotate about the same vertical axis with angular velocities ω_D, and ω_F, respectively. The Kármán boundary-layer (the rotating-disk boundary-layer flow described by Faller[1]) arises when the disk rotates and the fluid is stationary, i.e., $\omega_D \neq 0$, $\omega_F = 0$, for the Ekman layer $\omega_D \approx \omega_F$, and for the Bödewadt layer $\omega_D = 0$, $\omega_F \neq 0$. Between these particular examples are flow in which both the fluid and the disk rotate, but with differing angular velocities. Although the model is valid for counter- and co-rotating systems, only co-rotating systems will be analysed here. To incorporate this range of conditions in one model, a "system rotation rate", Ω, is defined by

$$\Omega = \frac{\omega_F}{2 - \mathrm{Ro}} + \frac{\omega_D}{2 + \mathrm{Ro}} \tag{1}$$

where Ro is the Rossby number, $\mathrm{Ro} = \Delta\omega/\Omega$, and $\Delta\omega$ is the difference of angular velocity, $\omega_F - \omega_D$. For the Kármán boundary-layer flows, it is given by $\Omega = \omega_D$, $\omega_F = 0$, $\mathrm{Ro} = -1$.

The component equations of motion for a uniform fluid in a cylindrical coordinate system rotating with the angular velocity ω_D may be written as

$$\overline{u}_t + (\overline{\boldsymbol{u}} \cdot \nabla)\overline{u} - \frac{\overline{v^2}}{r} - 2\omega_D \overline{v} = -\overline{p}_r + \nu\left(\nabla^2 \overline{u} - \frac{\overline{u}}{r^2} - \frac{2\overline{v}_\theta}{r^2}\right) \tag{2a}$$

$$\overline{v}_t + (\overline{\boldsymbol{u}} \cdot \nabla)\overline{v} - \frac{\overline{uv}}{r} + 2\omega_D \overline{u} = -\frac{\overline{p}_\theta}{r} + \nu\left(\nabla^2 \overline{v} - \frac{\overline{v}}{r^2} + \frac{2\overline{u}_\theta}{r^2}\right) \tag{2b}$$

$$\overline{w}_t + (\overline{\boldsymbol{u}} \cdot \nabla)\overline{w} = -\overline{p}_z + \nu\nabla^2 \overline{w} \tag{2c}$$

The continuity equation is

$$\frac{(r\overline{u})_r}{r} + \frac{\overline{v}_\theta}{r} + \overline{w}_z = 0 \tag{3}$$

where the subscripts t, r, θ and z denote partial differentiation.

Also, $\overline{u}$, $\overline{v}$ and $\overline{w}$ are the components of the velocity of the $\overline{\boldsymbol{u}}$ in the r, θ and z directions, respectively, the constant specific gravity is included with the pressure as p.

The dependent variates are separated into those of a basic flow (capitals) and fluctuations, as

$$(\overline{u}, \overline{v}, \overline{w}, \overline{p}) = (U, V, W, P) + (u, v, w, p) \tag{4}$$

Assuming an axially symmetrical similarity solution to the basic flow with the similarity variates $F(z, t)$, $G(z, t)$ and $H(z, t)$ defined by

$$\begin{aligned} U &= \Delta\omega r F(z) \\ V &= \Delta\omega r G(z) \\ W &= \Delta\omega D H(z) \end{aligned} \tag{5}$$

where $D=(\nu/\Omega)^{1/2}$ is the boundary-layer thickness, $t^*(=t/\Omega)$ is the non-dimensional time divided by Ω and $z^*(=z/D)$ is the non-dimensional axial coordinates which star (*) have been omitted for convenience.

The non-dimensional radial basic flow equation is

$$F_t+\mathrm{Ro}(F^2+HF_z-G^2)-\frac{2\omega_D}{\Omega}G=-\frac{P_r}{\Delta\omega rD\Omega}+F_{zz} \tag{6}$$

where $2\omega_D/\Omega\equiv\mathrm{Co}=2-\mathrm{Ro}-\mathrm{Ro}^2$, Coriolis parameter, and $P_r/\Delta\omega rD\Omega=P_r^*$ is suitably defined non-dimensional pressure whose radial gradient can be determined from the relative tangential flow as $z\to\infty$. Therefore $V=\Delta\omega r$, and $F=F_z=F_{zz}=0$, so $P_r^*=\mathrm{Ro}+\mathrm{Co}$.

The axial basic flow equation is $P_z/\Delta\omega D^2\Omega=P_z^*$, and from the continuity equation is $P_z^*=0$. Then the basic flow equations with respect to radial and tangential direction are

$$F_t+\mathrm{Ro}[F^2+HF_z-(G^2-1)]-\mathrm{Co}(G-1)-F_{zz}=0 \tag{7a}$$

$$G_t+\mathrm{Ro}(2FG+HG_z)+\mathrm{Co}F-G_{zz}=0 \tag{7b}$$

From equation (3) one obtains

$$H=-2\int_0^z F(z)\,dz \tag{8}$$

and boundary conditions are

$$F(0)=G(0)=H(0)=0,\quad F(\infty)=0,\quad G(\infty)=1 \tag{9}$$

2.2 The linear stability equations

Now the evolution of infinitesimally small disturbances imposed on the steady flow governed equations (2)~(3). The linear stability equations for the Kármán boundary-layer can be derived and reduced to the similarity form as was done by Faller et al.[14] (see also Faller[1]). We follow the way of Faller to reformulate the stability equations as below. But, our stability equations are slightly different compared to those of Faller. Namely, the present stability equations have been reformulated not only by correcting some errors but by keeping convective terms, instead of neglecting the perturbated terms with respect to r. Both the errors and neglected terms are appeared in the equation (30) of Faller et al.[14]

The conversion from cylindrical (r,θ)- to rotated rectangular $(\hat{x},\hat{y})$-coordinates by rotation through the angle $\delta=\varepsilon+(\pi/2)$ as illustrated in Fig. 2, where ε is the angle of the new $\hat{x}$-axis with respect to the tangential direction.

The perturbation equation oriented by the new $(\hat{x},\hat{y})$-coordinates which was rotated through the angle ε from the (x,y)-coordinates as was done by Faller[1] are then

$$u_t+\mathrm{Re}[-(FC+GS)u_y+(-F_zS+G_zC)w]+\mathrm{Ro}(Hu_z+Fu-2Gv)-\mathrm{Co}v=u_{yy}+u_{zz} \tag{10}$$

The reason why we choose the new oriented coordinates is very convenient to express with one-dimensional coordinates which the cross-flow instability has an azimuth angle ε relative

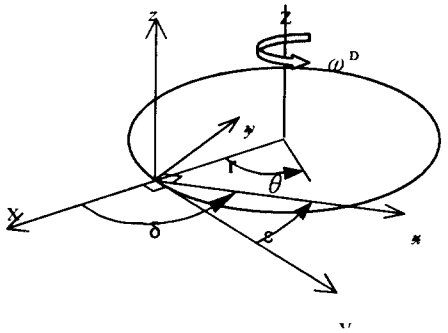

Fig. 2 Rotation system.

to the outer drawn radius tangentially.

The radial- and tangential-components of perturbation vorticity equations with respect to r-, θ-directions are denoted as ξ, η

$$\begin{aligned}&\xi_t+\mathrm{Re}\left(F\xi_r+\frac{G\xi_\theta}{r}-F_z v_r\right.\\&\quad+G_z u_r-wG_{zz})+\mathrm{Ro}(H\xi_z+H_z\xi\\&\quad-F_z v-Fv_z-2G_z u-2Gu_z+\frac{Fw_\theta}{r}\\&\quad\left.+G_z u\right)-\mathrm{Co}\,u_z=\nabla^2\xi-\frac{v_z}{r^2}-\frac{2u_{\theta z}}{r^2}\end{aligned}\tag{11a}$$

$$\begin{aligned}&\eta_t+\mathrm{Re}\left(F\eta_r+\frac{G\eta_\theta}{r}-\frac{F_z v_\theta}{r}\right.\\&\quad\left.+\frac{G_z u_\theta}{r}+wF_{zz}\right)+\mathrm{Ro}(H_z\eta+H\eta_z\\&\quad+F_z u+Fu_z-2G_z v-2Gv_z\\&\quad-Fw_r-\frac{Gw_\theta}{r}-F_z u+\frac{Gw_\theta}{r})\\&\quad-\mathrm{Co}\,v_z=\nabla^2\eta-\frac{u_z}{r^2}-\frac{2v_{\theta z}}{r^2}\end{aligned}\tag{11b}$$

To adopt a local rectangular coordinate system centered at some fixed value of Re let $dr\rightarrow dx$ and $rd\theta\rightarrow dy$. The rectangularized horizontal-component vorticity equations over the rotating disk, derived from equation (11), are then

$$\begin{aligned}&\xi_t+\mathrm{Re}(F\xi_x+G\xi_y-F_z u_x+G_z u_x\\&\quad-G_{zz}w)+\mathrm{Ro}(H\xi_z+H_z\xi\\&\quad-F_z v-Fv_z-2G_z u-2Gu_z+G_z u)\\&\quad-\mathrm{Co}\,u_z=\nabla^2\xi+\frac{v_z}{r^2}-\frac{2}{r}u_{yz}\end{aligned}\tag{12a}$$

$$\begin{aligned}&\eta_t+\mathrm{Re}(F\eta_x+G\eta_y-F_z v_y\\&\quad+G_z u_y+F_{zz}w)+\mathrm{Ro}(H_z\eta+H\eta_z\\&\quad+F_z u+Fu_z-2G_z v-2Gv_z\\&\quad-Fw_x-Gw_y-F_z u+Gw_y)\\&\quad-\mathrm{Co}\,v_z=\nabla^2\eta-\frac{u_z}{r^2}-\frac{2}{r}v_{yz}\end{aligned}\tag{12b}$$

where $\mathrm{Re}(=\Delta\omega\bar{r}D/\nu)$ is the Reynolds number.

Note that for the Kármán boundary-layer, since $\mathrm{Re}=\Delta\omega r/\Omega$, $\Delta\omega=-\omega_D$, $\Omega=\omega_D$, so $\mathrm{Re}=-r$ and is negative. But for convenience Re will be generally treated as a positive number. The instabilities are assumed to be 2-dimensional vortices independent of new $\hat{x}$-direction, so in the rotated equations $\partial/\partial\hat{x}=0$. The viscous terms $1/r$ and $1/r^2$ have been omitted because $1/r=-1/\mathrm{Re}$.

The perturbation vorticity equation oriented by the new $(\hat{x},\hat{y})$-coordinates which was rotated through the angle ε from the (x,y)-coordinates as was done by perturbation equation are then

$$\begin{aligned}&\xi_t+\mathrm{Re}[-(FC+GS)\xi_y+(F_{zz}C+G_{zz}S)w]\\&\quad+\mathrm{Ro}[H\xi_z+H_z\xi-Fv_z-F_z v-2G_z u\\&\quad-2Gu_z+(F_z C+G_z S)(uS+vC)\\&\quad+(FS-GC)w_y S+(GC-FS)w_y C]\\&\quad-\mathrm{Co}\,u_z=\xi_{yy}+\xi_{zz}\end{aligned}\tag{13}$$

The corrected sign term is $(GC-FS)$ and the whole convective terms kept $\mathrm{Ro}(F'C+G'S)\Phi'$, $\mathrm{Ro}S(F'C+G'S)U$ and $\mathrm{Ro}k^2S(FS-GC)$ are included.

The stream function for the flow in the new $(\hat{y},\hat{z})$-plane is defined by

$$w=\frac{\partial\phi}{\partial y},\quad v=-\frac{\partial\phi}{\partial z},\quad \xi=\nabla^2\phi\tag{14}$$

where $\hat{}$ is omitted for convenience.

The perturbation velocity u and stream function ϕ may be assumed as

$$u(y,z,t)=U(z)\exp[i(ky-\beta t)]\tag{15a}$$

$$\phi(y,z,t)=\Phi(z)\exp[i(ky-\beta t)]\tag{15b}$$

We shall immediately take advantage of linearity and seek solutions in terms of complex functions. In this way we will be able to re-

duce our system of partial differential equation (10) to ordinary differential equations, producing an obviously facility in the analysis. Thus real and imaginary parts, we find

$$\begin{aligned} U_R'' = {} & \mathrm{Ro}HU_R' + (\mathrm{Ro}F + k^2)U_R \\ & + [\beta + \mathrm{Re}(FC + GS)k]U_I \\ & + (2\,\mathrm{Ro}G + \mathrm{Co})\Phi_R' \\ & - \mathrm{Re}k(-F'S + G'C)\Phi_I \end{aligned} \tag{16a}$$

$$\begin{aligned} U_I'' = {} & \mathrm{Ro}HU_I' + (\mathrm{Ro}F + k^2)U_I \\ & - [\beta + \mathrm{Re}(FC + GS)k]U_R \\ & + (2\,\mathrm{Ro}G + \mathrm{Co})\Phi_I' \\ & + \mathrm{Re}k(-F'S + G'C)\Phi_R \end{aligned} \tag{16b}$$

The reformulated stability equation (13) with perturbation velocity and stream function equation (14) and (15) are complex-valued, 6th-order, linear system of homogeneous differential equations.

$$\begin{aligned} \Phi_R'''' = {} & \mathrm{Ro}H\Phi_R''' + (\mathrm{Ro}H' + \mathrm{Ro}F + 2k^2)\Phi_R'' \\ & + \mathrm{Ro}[F' - Hk^2 - C(F'C + G'S)]\Phi_R' \\ & - [\mathrm{Ro}H'k^2 + \mathrm{Ro}k^2S(FS - GC) \\ & + \mathrm{Ro}k^2C(GC - FS) + k^4]\Phi_R \\ & + [\beta + \mathrm{Re}(FC + GS)k]\Phi_I'' \\ & - [\beta k^2 + \mathrm{Re}(FC + GS)k^3 \\ & + \mathrm{Re}(F''C + G''S)k]\Phi_I \\ & - (2\,\mathrm{Ro}G + \mathrm{Co})U_R' \\ & + \mathrm{Ro}[S(F'C + G'S) - 2G']U_R \end{aligned} \tag{17a}$$

$$\begin{aligned} \Phi_I'''' = {} & \mathrm{Ro}H\Phi_I''' + (\mathrm{Ro}H' + \mathrm{Ro}F + 2k^2)\Phi_I'' \\ & + \mathrm{Ro}[F' - Hk^2 - C(F'C + G'S)]\Phi_I' \\ & - [\mathrm{Ro}H'k^2 + \mathrm{Ro}k^2S(FS - GC) \\ & + \mathrm{Ro}k^2C(GC - FS) + k^4]\Phi_I \\ & - [\beta + \mathrm{Re}(FC + GS)k]\Phi_R'' \\ & + [\beta k^2 + \mathrm{Re}(FC + GS)k^3 \\ & + \mathrm{Re}(F''C + G''S)k]\Phi_R \\ & - (2\,\mathrm{Ro}G + \mathrm{Co})U_I' \\ & + \mathrm{Ro}[S(F'C + G'S) - 2G']U_I \end{aligned} \tag{17b}$$

In order to specify the problem completely, boundary conditions are applied to the eigenfunction $(U(\eta), \Phi(\eta))$. Evidently, the velocity disturbances quantities u, v and w must be zero at the rotating disk surface and at a large distance out $(\eta \to \infty)$. Therefore, the non-dimensional boundary conditions are:

$$\begin{aligned} & U(0) = \Phi(0) = \Phi'(0) = 0 \\ & U'(\infty) = \Phi(\infty) = \Phi''(\infty) = 0 \end{aligned} \tag{18}$$

2.3 Numerical method

The boundary value problem, equations (16), (17) and (18) can be solved by using the technique of simple shooting from $\eta = \eta_\infty$, where it is the asymptotic solution valid as $\eta \to \infty$, to $\eta = 0$ and one seeks to satisfy the conditions in equation (18) that apply at $\eta = 0$ (Hwang[15]). Also, this problem can be solved by using the finite difference method (FDM) adopted the Adams-Bashforth time-step, centered difference in z as did Faller.[1] To reduce error propagation and to avoid the inaccuracies in both methods, the orthogonal collocation method is employed to solve the problem. Thus, our results were obtained primarily by using a two-point boundary value problem code COLNEW[16] that was based upon the adaptive orthogonal collocation method using B-spline. For the approximation of η_∞ in equation (18), $\eta_\infty = 40 \sim 120$ was chosen that was the same value for the base flow.

To generate the families of solutions, an *ad hoc* scheme was used as described below. Since there is no simple way to normalize the solutions of the eigenvalue problem, equations (16), (17) and (18) which has all homogeneous boundary conditions, an alternative must be found to avoid the trivial solution.

The boundary conditions, equation (18) are modified slightly and changed significantly. These conditions are expressed in the real and imaginary parts,

$$U_R(0)=U_I(0)=\Phi_R(0)=\Phi_I(0)=0 \qquad (19a)$$
$$\Phi_R'''(0)=\Phi_I'''(0)=J$$

$$U_R'(\infty)=U_I'(\infty)=\Phi_R(\infty)=\Phi_I(\infty)=0 \qquad (19b)$$
$$\Phi_R''(\infty)=\Phi_I''(\infty)=0$$

with $10^{-3}\leq|J|\leq 10^{-1}$.

The computing procedure employed to use the orthogonal collocation code COLNEW for obtaining the neutral stability curve is quite similar to that employed in simple shooting. For a given value Re, one guesses a pair of eigenvalues k and β. One then solves the linear stability equations (16) and (17) with the modified boundary conditions equation (19) replacing $\Phi'(0)=0$ using COLNEW, and iterates by adjusting the values of k and β until the boundary conditions $\Phi_R'(0)=\Phi_I'(0)=0$ are satisfied with $|\Phi_R'(0)|+|\Phi_I'(0)|\leq 10^{-6}$.

In our calculation, the following criteria was used to get the acceptable solution.

$$\min_{0\leq\eta\leq\infty}\left(\frac{|\Phi_R'(0)|}{|\Phi_R'(\eta)|},\frac{|\Phi_I'(0)|}{|\Phi_I'(\eta)|}\right)\leq 10^{-4} \qquad (20a)$$

$$\max\left(\frac{|\Phi_R'(0)|}{M},\frac{|\Phi_I'(0)|}{M}\right)\leq 10^{-7} \qquad (20b)$$

where M was maximum value of the eigenvector components (i.e., U, U', Φ, Φ', Φ'') on $0\leq\eta\leq\eta_\infty$. In addition, the error estimates given on output by COLNEW were less than 10^{-5}.

3. Results and discussion

3.1 Theoretical analysis

The reformulated stability equations by correcting sign error and by keeping whole convective terms are accurately solved by using the orthogonal collocation technique. As the results, the critical Reynolds number, wave number, and azimuth angle was obtained, but, the flow instability is not observed at that point. The flow instability, which was amplified and developed from the neutral stability condition, appears at the several times of critical Reynolds number to the stream flow.

The instability, which appears in the form of stationary spiral vortices at large Reynolds number and positive azimuth angle relative to circles on a disk, is Type I. Whereas Type II as well as Type I has a form of spiral vortices (Type II) has the opposite angle at the lower value of Re_c compared to Type I. More of, the vortices move rapidly outward and amplify as they progress. Using the reformulated equation, we obtained a critical Reynolds number $\mathrm{Re}_{c,1}=270$, as was shown in Table 1, which is in good agreement with the theoretical results of Faller[1] and Malik,[6] but is slightly less than the previous calculated values. The Type II instability in the Kármán boundary-layer like the Tollmien-Schlichting waves amplifies as it moves toward larger Re. But the Type II instability of three-dimensional boundary-layers should not be confused with or referred to as a Tollmien-Schlichting instability.

Not long ago, Malik,[6] Wilkinson and Malik,[8] Malik et al.,[13] and Mack[17] have shown that experimental and numerical studies for the Kármán boundary-layer are in approximate agreement and have converged on the value $\mathrm{Re}_{c,1}=290\pm 20$.

Similarilly, Malik et al.[13] was briefly mentioned that there appeared to be a critical value for Type II moving disturbances for the Ekman boundary-layer at $\mathrm{Re}_{c,2}=49$, but further information on that instability was not provided.

In this paper, a summery of new numerical calculations of the instabilities over a rotating disk presents in Tables 1 and 2. The critical Reynolds number of Type II instability has $\mathrm{Re}_{c,2}=37$, $k_{c,2}$ (wave number at $\mathrm{Re}_{c,2}$) $=0.385$

Table 1 Critical values of Type I instability

Mode	Type I		
	Faller[1]	Modified	Present
Re_c	285.3	270.8	270.2
k	0.378	0.389	0.386
ε	13.9	13.0	13.3
Cp		−4.44	−5.13

Table 2 Critical values of Type II instability

Mode	Type II		
	Faller[1]	Modified	Present
Re_c	69.4	38.25	36.9
k	0.279	0.355	0.385
ε	−19.0	−26.0	−23.5
Cp		17.70	15.79

and $\varepsilon_{c,2}$ (azimuth angle at $Re_{c,2}$) = −23.5°. Also, a comparison of the new numerical calculation with keeping whole convective terms and the modified calculation with correcting terms of Faller's form is shown in Tables 1 and 2.

Faller[1] obtained the neutral stability results $Re_{c,2}$=69.4, $k_{c,2}$=0.279 and $\varepsilon_{c,2}$=−19° for Type II instability. However, both results agree within resonable limits, not only considering the terms of linear stability equations he formulated are different with those of the present work, but the numerical techniques he employed are not as powerful as those available to the authors. Some numerical values of the available data are slightly different due to different stability equations and numerical scheme. It is impossible to compare directly the critical values of present work as well as other works with experimental data (see like Fig. 1). For the small critical Reynolds number of Type II instability, there are some doubtful reasons to adopt the parallel assumption for the linear stability equation to the entrance region.

Nevertheless, the azimuth angle which has ε = −15° at Re=352 for the experimental data (see Fig. 1) has negative value (−23.5°) according to the coordinates system (see Fig. 2), it can be considered the amplification rate and mechanism process corresponding to the change of azimuth angle. From the present work, the flow instability will arise at much less Reynolds number under parallel assumption than previously known results, also, the range of azimuth angle for the disturbances was broaden.

The Type II and secondary instability of Kármán boundary-layer which was abruptly rotating disk in a quiescent fluid illustrated photo from Faller[1] and sketch of their structured in Fig. 1. This figure is the one of the serial films in which the azimuth angle of Type II instability is moving outward from the center with ε = −15° and the secondary instability showed a specific mechanism for transition to turbulence that involved ribs with ε = 40° formed nearly perpendicular to the primary instability. In this picture, what the difference of the direction of $\hat{y}$ axis and that in Fig. 2 corresponding to the using Re for increased r in the stability calculation instead of −Re for convenience is outward direction from the rotating center in Fig. 1. For example, the disturbance amplified at r=61.4 cm (Re=352) and ε = −15°.

To explain the process of flow instability and transition, it need to draw the spatial and

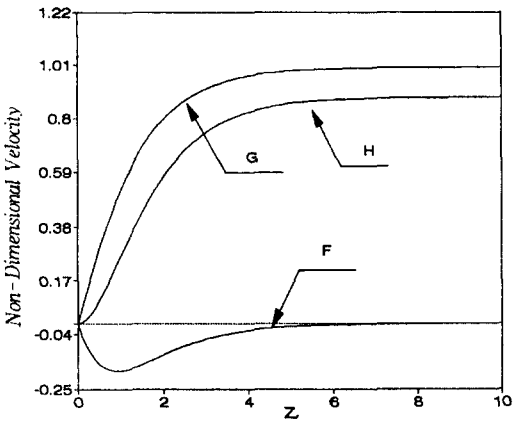

Fig. 3 Numerical solution of base flow equations for Ro = −1, Co = 2.

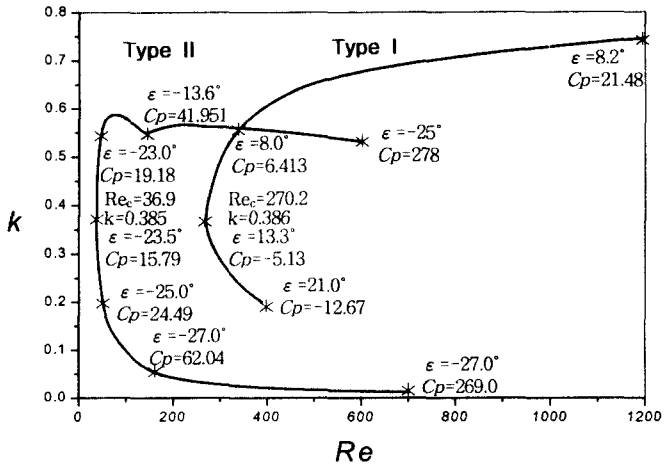

Fig. 4 4-dim. neutral stability curves for the Kármán boundary layer, corresponding to the Type I and II instabilities.

temporal amplification contour corresponding to the disturbances growing and decaying. The secondary instability was not considered. Non-dimensional velocity distribution for the base flow is shown in Fig. 3 and has an inflection point for the absolutely unstable.

The 4-dimensional neutral stability curves in Fig. 4 were drawn by connecting the most outer portions of stability curves from Figs. 5~11. The Flow is unstable in the inner region of these 4-dimensional curves but stable in the outer region. It was obtained 4-dimensional neutral stability curves, corresponding to the Type I and Type II in Fig. 4, and minimum values on the neutral curves of Type I instability near 'nose' in Table 3. Then, the wave velocity (Cp) is changed their sign for the flow condition. It is supposed that there is a stationary disturbance between these conditions because of wave velocity implies $Cp=0$. Comparison of neutral stability curves in the (Re, k)-plane for $\varepsilon=10°$ and 15° between present and previous known numerical results are in Fig. 5.

Table 3 Minimum values on the neutral curve of Type I instability near *'nose'*

Re_c	k	ε	Cp
385.19	0.6	8.5	9.74
297.69	0.5	10.1	2.50
270.61	0.4	12.8	−4.08
270.22	0.386	13.3	−5.13
288.84	0.3	16.3	−10.91
340.0	0.234	18.5	−14.67
388.36	0.2	19.1	−14.28
400.0	0.193	19.0	−63.30

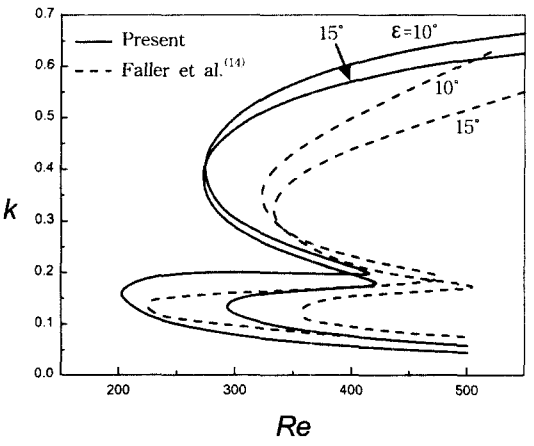

Fig. 5 Comparison of neutral stability curves in the (Re, k)-plane for $\varepsilon=10°$ and 15° between present and previous known numerical results.

The present work has less critical Reynolds number and slightly wide range of wave number than previous, and stationary disturbances will observed within this range of azimuth angle. The present stability results show that the flow becomes first unstable near the position of $Re_{c,1}=270.2$ for a disturbance wave of $k_{c,1}=0.386$ with $\varepsilon_{c,1}=13.3°$. Note that Cp is positive as $\varepsilon \rightarrow 8.2°$, whereas Cp is negative as $\varepsilon \rightarrow 21°$ and Cp is positive as k is larger upper part whereas Cp is negative as k is smaller lower part (see Fig. 4 and partly Table 3). Thus, it is expected that the value of ε tends to be slightly decreased from $\varepsilon=13.3°$ towards 8.2° as Re is further increased from $Re_{c,1}$ (see Hwang and Lee[18]). The above prediction reasonably agrees with the experimental data of Kobayashi et al.[2]

Neutral stability curves in the (Re, k)-, (Re, β)-, and (Re, Cp)-plane for the various azimuth angles are shown in Figs. 6, 7, and 8 and curve for $\varepsilon=-15°$ is shown in Figs. 9, 10, and 11. The positive wave frequency (β) mean that the direction of wave velocity (Cp)

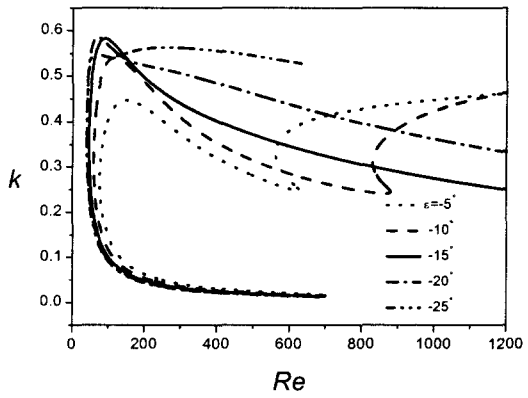

Fig. 6 Neutral stability curves in the (Re, k)-plane for $\varepsilon=-25°$, $-20°$, $-15°$, $-10°$ and $-5°$.

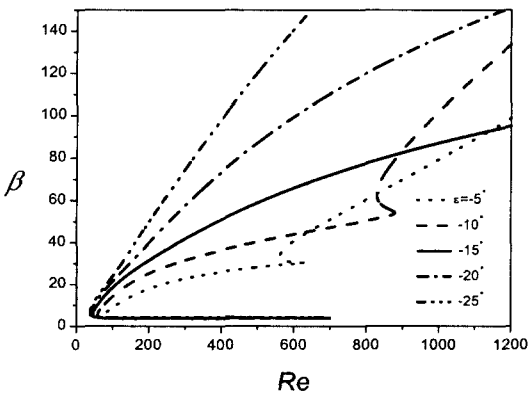

Fig. 7 Neutral stability curves in the (Re, β)-plane for $\varepsilon=-25°$, $-20°$, $-15°$, $-10°$ and $-5°$.

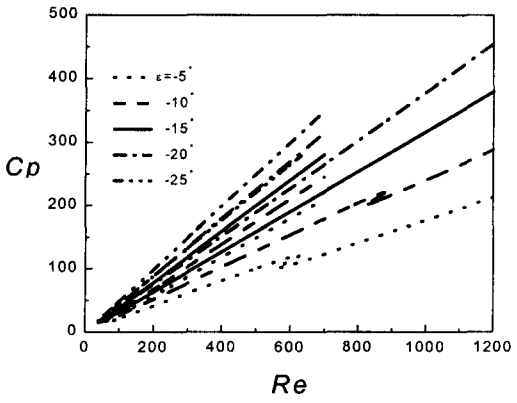

Fig. 8 Neutral stability curves in the (Re, Cp)-plane for $\varepsilon=-25°$, $-20°$, $-15°$, $-10°$ and $-5°$.

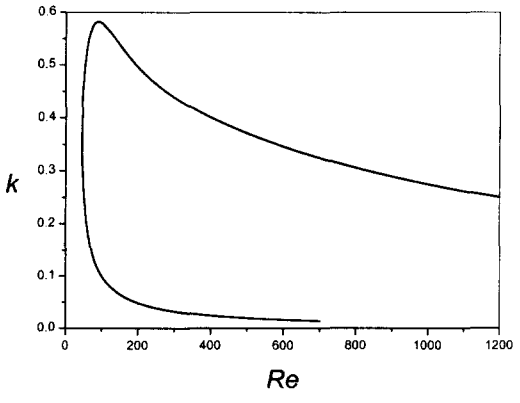

Fig. 9 Neutral stability curve in the (Re, k)-plane for $\varepsilon=-15°$.

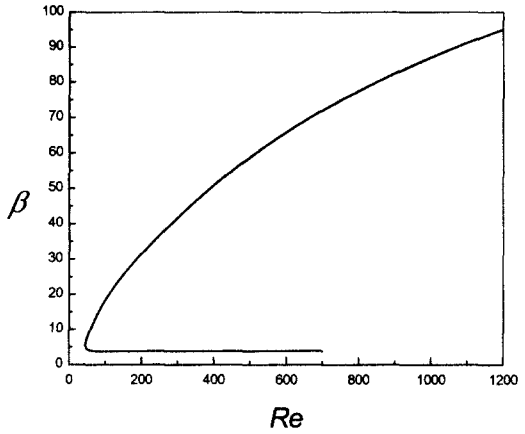

Fig. 10 Neutral stability curve in the (Re, β)-plane for $\epsilon = -15°$.

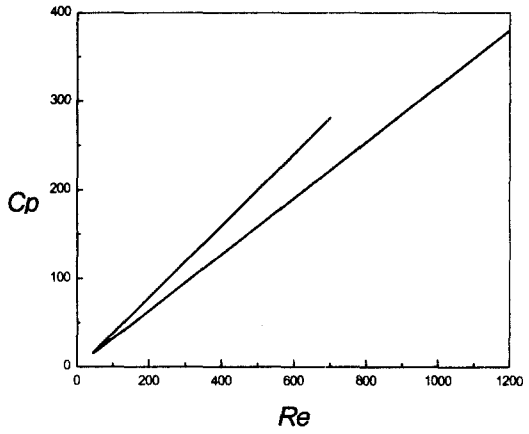

Fig. 11 Neutral stability curve in the (Re, Cp)-plane for $\epsilon = -15°$.

run parallel with the $\hat{y}$ axis in the coordinates system of Fig. 2.

3.2 Comparison with experimental data

Gregory et al.[11] discussed the application to swept-back airfoils, performed well-controlled experiments to find critical values of the Reynolds numbers for instability (Re_c) and for transition (Re_t) and developed a partial theory showing that those vortices were associated with an inflection point in the cross-vortex basic flow. They observed a stationary vortex pattern consisting of about 30 vortices between Reynolds numbers of 430 and 530. Kohama and Suda[3] observed that the number of spiral vortices is 33 or 35. Kobayashi et al.[2] calculated the value of $Re_{c,1}$ as 261 and observed that the number of spiral vortices is 31 or 32 at the position of $Re \simeq 297$. Faller[1] obtained the neutral stability results, e.g., $Re_{c,1}=285.3$, $k_{c,1}$ (wave number at $Re_{c,1}$)$=0.378$ and $\varepsilon_{c,1}$ (azimuth angle at $Re_{c,1}$)$=13.9°$ for Type I instability, while $Re_{c,2}=69.4$, $k_{c,2}=0.279$ and $\varepsilon_{c,2}=-19°$ for Type II instability. For the instability problem, the difference between experiment and calculation for the critical condition is agreeable with reasonable limits since this flow-field was sophisticated and had still many unsolved problems.

There are many methods measuring the number of the disturbances, like visualization, acoustics, and hot-wire techniques. But, there are not so many numerical and experimental results for Type II instability in the Kármán boundary-layer. Lilly[4] calculated numerical solutions of the Ekman layer problem. He found that the critical Reynolds number for the fast-moving disturbances is 55 and the orientation angle at the critical point is $-23°$, which decreases in magnitude as the Reynolds number increases. For Type II instability, a similar instability mechanism was detected in the experiments of Faller and Kaylor[10] and Tatro and Mollö-Christensen.[19]

The sequence of Fig. 1 shows the appearance of the secondary instability (ribs) in a series of three bands of dye as they move outward and undergo transition. Although the ribs are nearly perpendicular to the Type II bands, on other occasions they have been observed at an angle closer to that expected of Type I. A proper theory of the secondary instability must consider the complex three-dimensional flow that is the sum of the basic

flow and the Type II instability. Faller[1] present numerical calculations of the instabilities over a rotating disk, emphasizing Type II, and a description of four plausible mechanisms of transition to turbulence. He recognized the mechanism selected in any particular experiment should depend upon the level of excitation of Type II by disturbances in the external flow.

In this paper, it is suggested that the critical values of Type II are $Re_{c,2}=36.9$, $k=0.385$, and $\varepsilon=-23.5°$ in 4-dimensional neutral stability curves for the Kármán boundary-layer as shown in Fig. 4.

Further studies for instability amplification are needed to interpret the instability mechanism, and to investigate the stability conditions by drawing instability amplification contours within the neutral curve.

4. Conclusions

The hydrodynamic instability of the Kármán boundary-layer flow has been numerically investigated by employing the linear stability theory and experimentally compared with prior data. The previously known stability equations of Faller[1] are reformulated by correcting the sign error and by keeping the whole convective terms. The reformulated stability equations are accurately solved by a two-point boundary value problem solving code. A computer code COLNEW, based on the orthogonal collocation was used for obtaining the neutral stability curve. The results include more complete 4-dimensional neutral stability curves corresponding to the Type I and II instabilities. The present stability equations are slightly different with those of Faller,[1] but our obtained results, in particular, on Type II instability are considerably different. However, both results agree within reasonable limit, considering both of characteristic shapes of neutral stability curves are almost same.

In conclusion, the small disturbances intends to be decayed for $Re < Re_c$ whereas they can be selectively amplified, at least, for $Re > Re_c$. When the present numerical results are compared with the previously known results, the value of critical Re corresponding to Type I is moved from $Re_{c,1}=285.3$ to 270.2 and the value corresponding to Type II is from $Re_{c,2}=$ 69.4 to 36.9, respectively. Also, the corresponding wave number is moved from $k_1=0.378$ to 0.386 for Type I; from $k_2=0.279$ to 0.385 for Type II. The results show that the flow is always stable for the disturbance whose wave number $k>0.75$. The first unstable condition for Type II instability mode is the band of wave numbers $0.0 \leq k \leq 0.587$ with azimuth angles $-28.4° \leq \varepsilon \leq -17.5°$. Also, the similar condition for Type I instability mode is $0.15 \leq k \leq 0.747$ with $8.0° \leq \varepsilon \leq 21°$.

The prediction from the present results on both instability modes excellently agrees with the previously known experimental data. In particular, it reasonably explains the previously observed subtle phenomena of Type I instabilities by considering the relation between the disturbance waves speeds and azimuth angles. This implies that the disturbances will be relatively fast amplified at small Re and within narrow bands of wave number compared with the previous results.

Acknowledgements

This paper was supported by 63 research fund at Sungkyunkwan University (1998), and partly by the Brain Korea 21 project.

References

1. Faller, A. J., 1991, Instability and Transition of Disturbed Flow over a Rotating Disk, J. Fluid Mech., Vol. 230, pp. 245-269.
2. Kobayashi, R., Kohama, Y. and Takamadate,

Ch., 1980, Spiral Vortices in Boundary Layer Transition Regime on a Rotating Disk, Acta Mechanica, Vol. 35, pp. 71-82.

3. Kohama, Y. and Suda, K., 1993, Crossflow Instability in a Spinning Disk Boundary Layer, AIAA Journal, Vol. 31, No. 1, pp. 212-214.
4. Lilly, D. K., 1966, On the Instability of Ekman Boundary Flow, J. of the Atmospheric Science, Vol. 23, pp. 481-494.
5. Lingwood, R. J., 1996, An Experimental Study of Absolute Instability of the Rotating Disk Boundary Layer Flow, J. Fluid Mech., Vol. 314, pp. 373-405.
6. Malik, M. R., 1986, The Neutral Curve for Stationary Disturbances in Rotating Disk Flow, J. Fluid Mech., Vol. 164, pp. 275-287.
7. Smith, N. H., 1947, Exploratory Investigation of Boundary Layer Oscillations on a Rotating Disk, NACA Tech. Note 1227.
8. Wilkinson, S. P. and Malik, M. R., 1983, Stability Experiments in the Flow over a Rotating Disk, AIAA Journal, Vol. 23, pp. 588-595.
9. Sparrow, E. M. and Gregg, J. L., 1960, Mass Transfer, Flow and Heat Transfer about a Rotating Disk, Transactions ASME, J. Heat Transfer, Vol. 82, pp. 294-302.
10. Faller, A. J. and Kaylor, R. E., 1966, A Numerical Study of the Instability of the Laminar Ekman Boundary Layer, J. Atmos. Sci., Vol. 23, pp. 466-480.
11. Gregory, N., Stuart, J. T. and Walker, W. S., 1955, On the Stability of Three-Dimensional Boundary Layers with Application to the Flow Due to a Rotating Disk, Phil. Trans. Roy. Soc., Vol. 248, pp. 155-199.
12. Gregory, N. and Walker, W. S., 1960, Experiments on the Effect of Suction on the Flow Due to a Rotating Disk, J. Fluid Mech., Vol. 9, pp. 225-234.
13. Malik, M. R., Wilkinson, S. P. and Orszag, S. A., 1981, Instability and Transition in Rotating Disk Flow, AIAA Journal, Vol. 19, No. 9, pp. 1131-1138.
14. Faller, A. J., Yang, S. T. and Piomelli, U., 1989, Instability of the KEB Boundary Layers, Tech. Note BN-1102, Inst. Phys. Sci. and Tech., U. of Maryland.
15. Hwang, Y-K, 1996, Stability of Buoyancy-Induced Flows Adjacent to a Vertical Isothermal Surface in Cold Pure Water, KSME Journal, Vol. 10, No. 4, pp. 498-508.
16. Bader, G. and Ascher, U., 1985, A New Basis Implementation for a Mixed Order Boundary O.D.E. Solver, Tech. Rep. 85-11, Dept. of Computer Science, U. of British Columbia, Vancouver, Canada.
17. Mack, L. M., 1985, The Wave Pattern Produced by Point Source on a Rotating Disk. AIAA Aerospace Science Meeting, Jan. 14-17, Reno, Nevada, AIAA Paper 85-0490.
18. Hwang, Y.-K. and Lee, Y.-Y., 1999, A Theoretical Flow Instability of the Kármán Boundary-Layer, Proceedings of the KSME 1999 Fall Annual Meeting B (Korean), pp. 737-742.
19. Tatro, P. R. and Mollö-Christensen, E. L., 1967, Experiments on Ekman Layer Instability, J. Fluid Mech., Vol. 28, pp. 531-543.